



# Magnesium ion-conducting solid polymer electrolyte based on cellulose acetate with magnesium nitrate ( $\text{Mg}(\text{NO}_3)_2 \cdot 6\text{H}_2\text{O}$ ) for electrochemical studies

M. Mahalakshmi<sup>1,2,3</sup> · S. Selvanayagam<sup>1</sup> · S. Selvasekarapandian<sup>2,4</sup> · M. V. Leena Chandra<sup>5</sup> · P. Sangeetha<sup>2,6</sup> · R. Manjuladevi<sup>2,7</sup>

Received: 15 September 2019 / Revised: 12 April 2020 / Accepted: 8 May 2020 / Published online: 1 June 2020  
© Springer-Verlag GmbH Germany, part of Springer Nature 2020

## Abstract

In this paper, the solution casting technique was used to develop the magnesium-conducting solid polymer electrolyte (PE) using cellulose acetate (CA) with the magnesium nitrate ( $\text{Mg}(\text{NO}_3)_2 \cdot 6\text{H}_2\text{O}$ ) salt. The crystalline/amorphous nature of CA with different concentrations of  $\text{Mg}(\text{NO}_3)_2 \cdot 6\text{H}_2\text{O}$  polymer electrolytes was studied by X-ray diffraction (XRD) analysis. The highest ionic conductivity of  $9.19 \times 10^{-4}$  S/cm was found for 60 wt.%CA/40 wt.%  $\text{Mg}(\text{NO}_3)_2 \cdot 6\text{H}_2\text{O}$  PE by Ac impedance spectroscopy at room temperature. The polymer membranes are subjected to FTIR analysis. The glass transition temperatures ( $T_g$ ) of the PEs were determined using differential scanning calorimeter (DSC). Then, the transference number of  $\text{Mg}^{2+}$  ion for 60 wt.%CA/40 wt.%  $\text{Mg}(\text{NO}_3)_2 \cdot 6\text{H}_2\text{O}$  PE was measured as 0.35 using Evan's method. The electrochemical stability of 3.65 V was observed for the highest ionic conducting PE by linear sweep voltammetry. The cyclic voltammetry (CV) study was done for highest ionic conducting polymer electrolyte. Finally, the primary magnesium battery was constructed with the highest ionic conducting PE, and its performance was studied.

**Keywords** Solution casting technique · Cellulose acetate · Magnesium nitrate · Ionic conductivity · Open-circuit voltage

## Introduction

The most challenging and ever-growing research area of solid-state ionics has attracted worldwide attention due to their vast applications in solid-state devices like rechargeable batteries,

sensors, supercapacitors, fuel cells, electrochemical solar cells, and electrochromic displays. Solid polymer electrolytes have certain advantages like no leakage, long-term structural stability, flexible geometry, good thermal, mechanical and electrical stability, good compatibility with electrodes, and safety [1]. Synthetic solid polymer electrolytes are having many disadvantages such as more expensive and non-degradable. To overcome these defects, biopolymer electrolytes have been used in various electrochemical devices. Biopolymers are chain-like molecules made up of repeating chemical blocks produced from renewable resources which are degraded in the environment. The non-toxic and biodegradable properties of biopolymers are boosting their applications in electronics and energy devices [2].

The main three classes of biopolymers are polynucleotides, polypeptides, and polysaccharides [3]. Cellulose acetate (CA) is one of the polysaccharide types, and it has many advantages. It is a modified natural polymer with a wide range of properties such as moderate flux, cost-effectiveness, relatively easy manufacture, renewable resource of raw material, and non-toxicity [4]. S.Z.Z. Abidin et al. have reported an electrochemical study on cellulose acetate-LiBOB polymer gel

✉ S. Selvasekarapandian  
sekarapandian@rediffmail.com

<sup>1</sup> PG& Research Department of Physics, Government Arts College Melur, Melur 625 106, India

<sup>2</sup> Materials Research Center, Coimbatore 641 045, India

<sup>3</sup> Department of Physics, Sri Meenakshi Government Arts College for Women(A), Madurai 625 002, India

<sup>4</sup> Department of Physics, Bharathiar University, Coimbatore 641 046, India

<sup>5</sup> Research Center of Physics, Fatima College, Madurai, India

<sup>6</sup> Department of Physics, Arulmigu Palaniandavar College of Arts and Culture, Palani, India

<sup>7</sup> Department of Physics, PSG college of Arts & Science, Coimbatore, India

electrolytes [5]. S. Monisha et al. have reported the study of CA with ammonium salts such as  $\text{NH}_4\text{SCN}$  and  $\text{NH}_4\text{NO}_3$ . She has also constructed the energy storage lithium battery using CA with  $\text{LiNO}_3$  [6–8]. Ramesh et al. have measured the highest ionic conductivity value of  $1.75 \times 10^{-3}$  S/cm for the sample CA/LiTFSI/[Amim] Cl (14 wt.%/6 wt.%/80 wt.%) [9]. Biodegradable polymer CA doped with lithium perchlorate ( $\text{LiClO}_4$ ) for supercapacitors has been reported by Selvakumar et al. [10]

Nowadays, magnesium-based batteries are trying to replace lithium-based rechargeable batteries due to the following advantages of low cost, abundances, safety, and also it has similar electrochemical properties of Li because it is placed next to the lithium in the periodic table [11]. Due to the divalent property,  $\text{Mg}^{2+}$  has the higher theoretical volumetric capacity ( $3832 \text{ mAh cm}^{-1}$ ) than Li ( $2062 \text{ mAh cm}^{-1}$ ). Therefore, magnesium batteries have more attention in recent years [12]. Pandey et al. have reported the studies on the effect of nano-sized MgO in magnesium ion-conducting gel polymer electrolytes polyvinylidene fluoride co-hexafluoropropylene (PVdF-HFP) for rechargeable magnesium batteries and reported maximum ionic conductivity of  $8 \times 10^{-3}$  S/cm for 3 wt.% of MgO at room temperature [13]. Manjuladevi et al. synthesize the blend polymer electrolyte based on poly(vinyl alcohol)-polyacrylonitrile with magnesium nitrate for magnesium battery and reported the maximum ionic conductivity of  $1.71 \times 10^{-3}$  S/cm for 92.5 wt.% PVA/7.5 wt.% PAN/0.3 wt.%  $\text{Mg}(\text{NO}_3)_2$  membrane [14]. The study of biopolymer I-carrageenan with magnesium perchlorate has been carried out by Shanmugapriya et al. and reported the ionic conductivity value of  $2.18 \times 10^{-3}$  S/cm at room temperature [15]. Eco-friendly biopolymer electrolyte using pectin with magnesium nitrate salt has been prepared by S. Kiruthika et al. and reported the highest ionic conductivity of  $7.70 \times 10^{-4}$  S/cm for 50 wt.% pectin/50 wt.%  $\text{Mg}(\text{NO}_3)_2$  at room temperature [16]. P. Sangeetha et al. have studied about the characterization of biopolymer K-carrageenan with  $\text{MgCl}_2$  and found the highest ionic conductivity value  $2.18 \times 10^{-3}$  for the sample of 1 g K-C/0.6 wt.% of  $\text{MgCl}_2$  [17].

Novelty of this paper, cellulose acetate (CA), is a semi-crystalline polymer derived from cellulose. It is not soluble in water. The chemical properties of CA are unique as a consequence of the presence of carboxyl groups (C=O) in their structure. CA has got a good film-forming property. According to the literature survey, it is observed that the study of magnesium with polymer CA is very scarce except one paper [18]. In this present work, magnesium ion-conducting polymer electrolytes are prepared using cellulose acetate and magnesium nitrate using DMF as a solvent by the solution casting technique. Then, the prepared membranes are subjected to various characterization techniques such as XRD, FTIR, DSC, Ac impedance, transport number study, LSV, and CV.

A primary magnesium battery has been constructed using the highest ionic conducting membrane and its performance is studied.

## Experimental technique

### Materials used

In this study, cellulose acetate (CA) and magnesium nitrate ( $\text{Mg}(\text{NO}_3)_2 \cdot 6\text{H}_2\text{O}$ ) were used as raw materials to prepare the polymer electrolytes by the solution casting technique, and dimethylformamide (DMF) was used as a solvent.

### Membrane preparation

In this work, different concentration of CA (Sigma-Aldrich with average  $M_n = 50,000$  by GPC, p.code: 1001345528) and  $\text{Mg}(\text{NO}_3)_2 \cdot 6\text{H}_2\text{O}$  (Hi-Media) were added with DMF solvent (Merck specialties Private Ltd., Mumbai, India) separately at room temperature and stirred continuously with a magnetic stirrer for several hours. Then, both the solutions were mixed well and stirred for several hours continuously to obtain a homogeneous solution. The obtained mixture was transferred into a polypropylene Petri dish and dried at  $60^\circ\text{C}$  to evaporate the solvent. It yielded a mechanically stable, transparent, and flexible film of thickness ranging from 180 to 200  $\mu\text{m}$ . Pure CA, 70 wt.% CA/30 wt.%  $\text{Mg}(\text{NO}_3)_2 \cdot 6\text{H}_2\text{O}$ , 60 wt.% CA/40 wt.%  $\text{Mg}(\text{NO}_3)_2 \cdot 6\text{H}_2\text{O}$  and 50 wt.% CA/50 wt.%  $\text{Mg}(\text{NO}_3)_2 \cdot 6\text{H}_2\text{O}$  electrolytes were prepared by this method, and films were stored in vacuum desiccators and used for various characterization techniques.

### Characterization

#### XRD analysis

The X-ray diffraction pattern of the polymer electrolytes was taken on the Shimadzu XRD 6000 X-ray diffractometer system using  $\text{CuK}\alpha$  radiation in the range of  $2\theta = 5^\circ$  to  $80^\circ$ .

#### Vibrational study

The polymer electrolytes were subjected to the FTIR measurement using the BRUCKER spectrometer in the wavenumber ranges from 700 to  $4000 \text{ cm}^{-1}$  with a resolution of  $1 \text{ cm}^{-1}$ .

#### Differential scanning calorimetry study

Glass transition temperature of the polymer electrolytes is measured using DSCQ20 V4.10 build 122 with a resolution of 0.01 mg. The films were taken in an aluminum pan and heated up to  $500^\circ\text{C}$  with a heating rate of  $5^\circ\text{C}/\text{min}$  under air-

controlled atmosphere, and during the measurements, the films were purged using a nitrogen atmosphere. Dry nitrogen gas at the rate of 50 ml/min was purged through the cell during the thermal treatment.

### Impedance study

The impedance of the polymer electrolytes was measured in the frequency range of 42 Hz to 1 MHz at room temperature using the HIOKI 3532-50LCR HiTESTER.

### Transference number measurement

The transference number of the  $Mg^{2+}$  ions for the highest conducting polymer electrolyte was measured using Evan's method, and Wagner's dc polarization method was used to find out the ionic and electronic transference number.

### Electrochemical stability studies

Electrochemical stability of the membrane was analyzed by linear sweep voltammetry using Biologic Science Instruments VSP-300, France. These cells were analyzed at a scan rate of 5 mV/s with a configuration of SS/polymer electrolyte/SS in the potential range of 0–5 V, and cyclic voltammogram has been recorded using Biologic Science Instruments VSP-300 by using highest conducting sample between –5 and +5 V at a scan rate of 1 mV/s.

### Primary Mg battery fabrication

A primary magnesium battery was constructed using the highest ionic conductivity membrane. Here, a magnesium metal plate acts as the anode and  $MnO_2$  with graphite and electrolyte in the ratio of 3:1:1 in the form of a pellet acts as the cathode. The performance of the primary magnesium battery has been studied.

**Preparation of anode** The magnesium metal of diameter 12 mm and the thickness 1 mm was prepared for the anode.

**Preparation of cathode** The required amount of manganese dioxide ( $MnO_2$ ), graphite, and highest ionic conducting electrolytes in 3:1:1 ratio was grained together and pressed with 5-ton pressure to form a pellet of diameter 12 mm.

## Results and discussion

### X-ray diffraction analysis

XRD measurements were carried out to investigate the amorphous/crystalline nature of the polymer electrolytes.

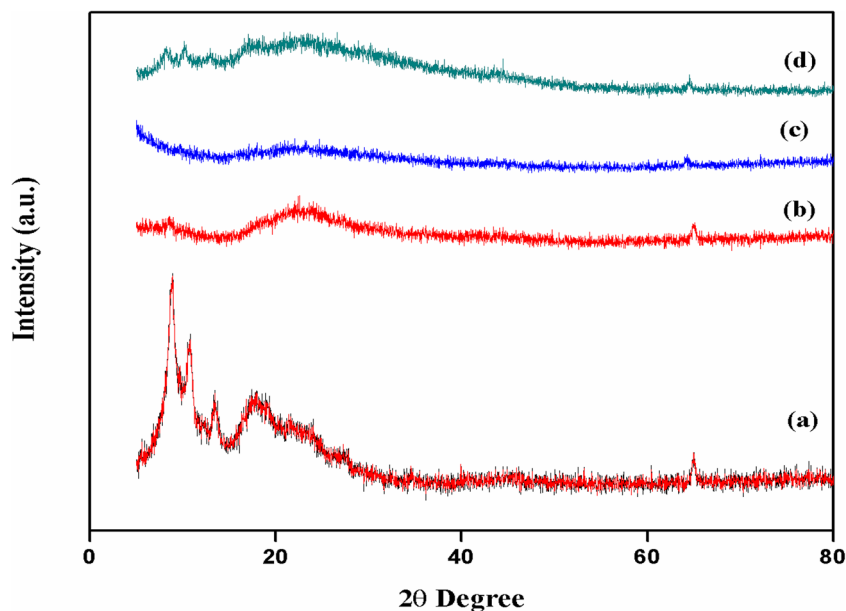
The XRD pattern for pure CA, 70 wt.% CA/30 wt.%  $Mg(NO_3)_2 \cdot 6H_2O$ , 60 wt.% CA/40 wt.%  $Mg(NO_3)_2 \cdot 6H_2O$ , and 50 wt.% CA/50 wt.%  $Mg(NO_3)_2 \cdot 6H_2O$  are shown in Fig. 1. The peaks observed at  $9^\circ$ ,  $11^\circ$ ,  $13^\circ$ , and  $18^\circ$  are the characteristic diffraction peaks of pure CA, which agree with previous research done by Ramesh et al. and Shuhaimi et al. [9, 19]. The peaks observed at  $9^\circ$ ,  $11^\circ$ , and  $13^\circ$  have vanished for 70 wt.% CA/30 wt.%  $Mg(NO_3)_2 \cdot 6H_2O$ , 60 wt.% CA/40 wt.%  $Mg(NO_3)_2 \cdot 6H_2O$ , and 50 wt.% CA/50 wt.%  $Mg(NO_3)_2 \cdot 6H_2O$  polymer electrolytes. The peak observed at  $18^\circ$  has become more broad, and less intense for 70 wt.% CA/30 wt.%  $Mg(NO_3)_2 \cdot 6H_2O$  polymer electrolyte, and it disappeared for polymer electrolyte 60 wt.% CA/40 wt.%  $Mg(NO_3)_2 \cdot 6H_2O$ , which implies that polymer membrane 60 wt.% CA/40 wt.%  $Mg(NO_3)_2 \cdot 6H_2O$  has become more amorphous in nature. The correlation between the intensity of peak and the degree of crystallinity is interpreted by Hodge et al. [20]. Furthermore, increasing the concentration of  $Mg(NO_3)_2 \cdot 6H_2O$  more than 40 wt.% ion aggregates formed, which reduces the number of charge carrier [21]. The peaks at  $9^\circ$ ,  $11^\circ$ ,  $13^\circ$ , and  $18^\circ$  are attributed to polymer CA that reappear for 50 wt.% CA/50 wt.%  $Mg(NO_3)_2 \cdot 6H_2O$  electrolyte as seen from the Fig. 1. This shows that amorphous nature decreases and crystalline nature increases for 50 wt.% CA/50 wt.%  $Mg(NO_3)_2 \cdot 6H_2O$  electrolyte.

### FTIR analysis

Fourier transform infrared (FTIR) spectroscopy analysis is a powerful tool to investigate the interaction between the host polymer and salt. Figure 2a, b, and c show the FTIR spectra of pure CA, 70 wt.% CA/30 wt.%  $Mg(NO_3)_2 \cdot 6H_2O$ , 60 wt.% CA/40 wt.%  $Mg(NO_3)_2 \cdot 6H_2O$  and 50 wt.% CA/50 wt.%  $Mg(NO_3)_2 \cdot 6H_2O$  polymer electrolytes in the range of  $700$ – $4000\text{ cm}^{-1}$ ,  $700$ – $1500\text{ cm}^{-1}$ , and  $1500$ – $1800\text{ cm}^{-1}$ , respectively, and the corresponding peak assignments are tabulated in Table 1.

A broad peak observed at  $3387\text{ cm}^{-1}$ , assigned to the stretching vibration of the hydroxyl groups ( $-OH$ ) of the pure CA, gets shifted to  $3378$ ,  $3358$ , and  $3369\text{ cm}^{-1}$  for 70 wt.% CA/30 wt.%  $Mg(NO_3)_2 \cdot 6H_2O$ , 60 wt.% CA/40 wt.%  $Mg(NO_3)_2 \cdot 6H_2O$ , and 50 wt.% CA/50 wt.%  $Mg(NO_3)_2 \cdot 6H_2O$  electrolytes, respectively. The change in the frequency of  $-OH$  stretching is due to the change of water content in the sample. The vibrational peak observed at  $1740\text{ cm}^{-1}$  in the pure CA assigned to  $C=O$  stretching in the carbonyl group of CA is decreased in intensity and also shifted to  $1737$ ,  $1735$ , and  $1732\text{ cm}^{-1}$  for 70 wt.% CA/30 wt.%  $Mg(NO_3)_2 \cdot 6H_2O$ , 60 wt.% CA/40 wt.%  $Mg(NO_3)_2 \cdot 6H_2O$ , and 50 wt.% CA/50 wt.%  $Mg(NO_3)_2 \cdot 6H_2O$  electrolytes, respectively. It is shown in Fig. 2c. This frequency shift is due to the interaction of  $Mg(NO_3)_2 \cdot 6H_2O$  with  $C=O$  as shown in Fig. 3 [22]. The peak at  $1646\text{ cm}^{-1}$  for 60 wt.% CA/40 wt.%  $Mg(NO_3)_2 \cdot 6H_2O$

**Fig. 1** XRD patterns of **a** pure CA, **b** 70 wt.% CA/30 wt.%  $\text{Mg}(\text{NO}_3)_2 \cdot 6\text{H}_2\text{O}$ , **c** 60 wt.% CA/40 wt.%  $\text{Mg}(\text{NO}_3)_2 \cdot 6\text{H}_2\text{O}$ , and **d** 50 wt.% CA/50 wt.%  $\text{Mg}(\text{NO}_3)_2 \cdot 6\text{H}_2\text{O}$



and 50 wt.% CA/50 wt.%  $\text{Mg}(\text{NO}_3)_2 \cdot 6\text{H}_2\text{O}$  polymer spectra is assigned to the OH bending. This is due to the water molecule. The medium intensity peak observed at  $1368\text{ cm}^{-1}$  in pure CA is attributed to C–H bending. Pure  $\text{Mg}(\text{NO}_3)_2 \cdot 6\text{H}_2\text{O}$  has shown FTIR spectrum at  $1347\text{ cm}^{-1}$  ascribed to asymmetric structure of  $\text{NO}_3^-$  ion [23]. In our case, FTIR peak due to  $\text{NO}_3^-$  ion overlaps with  $1368\text{ cm}^{-1}$  peak assigned to C–H bending due to CA. It is observed that, as the concentration of  $\text{Mg}(\text{NO}_3)_2 \cdot 6\text{H}_2\text{O}$  increases, due to interaction, the peak intensity decreases and also shifted to  $1369$ ,  $1371$ , and  $1374\text{ cm}^{-1}$  for 70 wt.% CA/30 wt.%  $\text{Mg}(\text{NO}_3)_2 \cdot 6\text{H}_2\text{O}$ , 60 wt.% CA/40 wt.%  $\text{Mg}(\text{NO}_3)_2 \cdot 6\text{H}_2\text{O}$ , and 50 wt.% CA/50 wt.%  $\text{Mg}(\text{NO}_3)_2 \cdot 6\text{H}_2\text{O}$  electrolytes, respectively. The absorption peak of pure CA at  $1221\text{ cm}^{-1}$  assigned to C–O stretching mode gets shifted towards increasing values as  $1227$ ,  $1228$ , and  $1247\text{ cm}^{-1}$  for 70 wt.% CA/30 wt.%  $\text{Mg}(\text{NO}_3)_2 \cdot 6\text{H}_2\text{O}$ , 60 wt.% CA/40 wt.%  $\text{Mg}(\text{NO}_3)_2 \cdot 6\text{H}_2\text{O}$ , and 50 wt.% CA/50 wt.%  $\text{Mg}(\text{NO}_3)_2 \cdot 6\text{H}_2\text{O}$  electrolytes, respectively.

The vibrational peak observed at  $1034\text{ cm}^{-1}$  in pure CA is assigned to C–O–C stretching vibration. As the concentration of  $\text{Mg}(\text{NO}_3)_2 \cdot 6\text{H}_2\text{O}$  increases, the intensity of the band decreases and also it gets shifted towards the values as  $1035\text{ cm}^{-1}$  and  $1037\text{ cm}^{-1}$  for 70 wt.% CA/30 wt.%  $\text{Mg}(\text{NO}_3)_2 \cdot 6\text{H}_2\text{O}$  and 60 wt.% CA/40 wt.%  $\text{Mg}(\text{NO}_3)_2 \cdot 6\text{H}_2\text{O}$  electrolytes, respectively. On further increase of concentration to 50 wt.%  $\text{Mg}(\text{NO}_3)_2 \cdot 6\text{H}_2\text{O}$ , the peak at  $1034\text{ cm}^{-1}$  split into two, one at  $1024\text{ cm}^{-1}$  and another at  $1076\text{ cm}^{-1}$  (Fig. 2b). This  $1076\text{ cm}^{-1}$  is due to  $\text{NO}_3^-$  symmetry stretching (pure  $\text{Mg}(\text{NO}_3)_2 \cdot 6\text{H}_2\text{O}$  symmetry stretching of  $\text{NO}_3^-$  ion appears at  $1058\text{ cm}^{-1}$  [24]). The medium intensity peak observed at  $906\text{ cm}^{-1}$  assigned to O–H bending vibrational mode to pure CA has been shifted to  $902$ ,  $900$ , and  $895\text{ cm}^{-1}$  for

70 wt.% CA/30 wt.%  $\text{Mg}(\text{NO}_3)_2 \cdot 6\text{H}_2\text{O}$ , 60 wt.% CA/40 wt.%  $\text{Mg}(\text{NO}_3)_2 \cdot 6\text{H}_2\text{O}$ , and 50 wt.% CA/50 wt.%  $\text{Mg}(\text{NO}_3)_2 \cdot 6\text{H}_2\text{O}$  electrolytes, respectively.

Shifting of peak frequency could be explained by calculating the force constant for pure membrane and membrane with salt. In this case for example,  $1221\text{ cm}^{-1}$  ascribed to C–O stretching has shifted to  $1227$ ,  $1228$ , and  $1247\text{ cm}^{-1}$  for 70 wt.% CA/30 wt.%  $\text{Mg}(\text{NO}_3)_2 \cdot 6\text{H}_2\text{O}$ , 60 wt.% CA/40 wt.%  $\text{Mg}(\text{NO}_3)_2 \cdot 6\text{H}_2\text{O}$ , and 50 wt.% CA/50 wt.%  $\text{Mg}(\text{NO}_3)_2 \cdot 6\text{H}_2\text{O}$  electrolytes, respectively. This increase in frequency has been explained by calculating the force constant. The following equation (1) is used to measure the force constant.

$$\bar{\nu} = \frac{1}{2\pi c} \sqrt{K/\mu} \quad (1)$$

where

- $\bar{\nu}$  is the wavenumber ( $\text{cm}^{-1}$ )
- $c$  is the velocity of light ( $3 \times 10^{10}\text{ cm/s}$ )
- $K$  is the force constant (Newton/cm)
- $\mu$  is the reduced mass which is given by

$$\mu = \frac{m_1 * m_2}{m_1 + m_2} \quad (2)$$

where  $m_1$  and  $m_2$  are the atomic masses of two atoms (C and O).

The force constant for C–O stretching vibration was calculated and tabulated in Table 2. It is found that the force constant values for all polymer electrolytes have increased slightly to

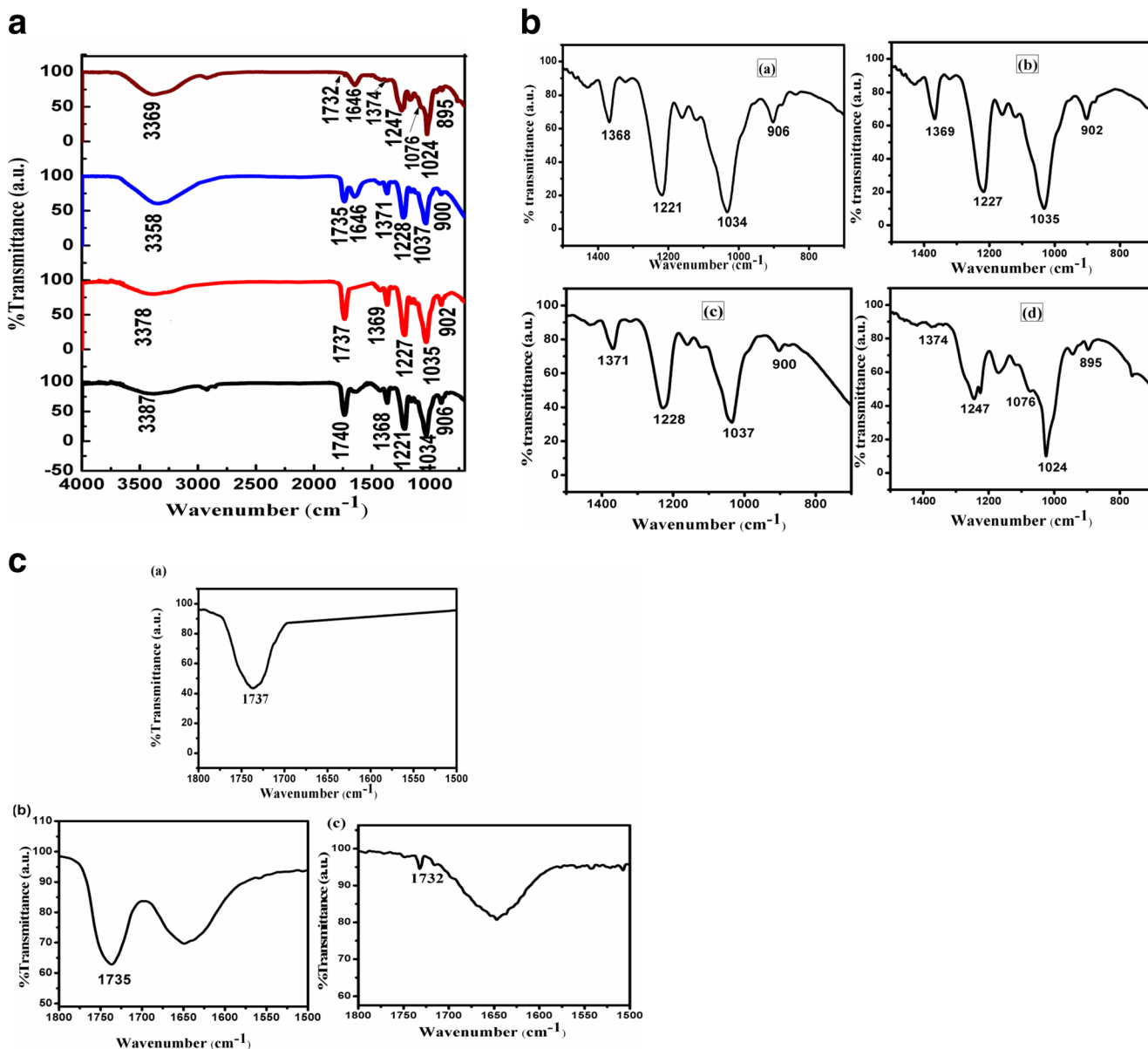
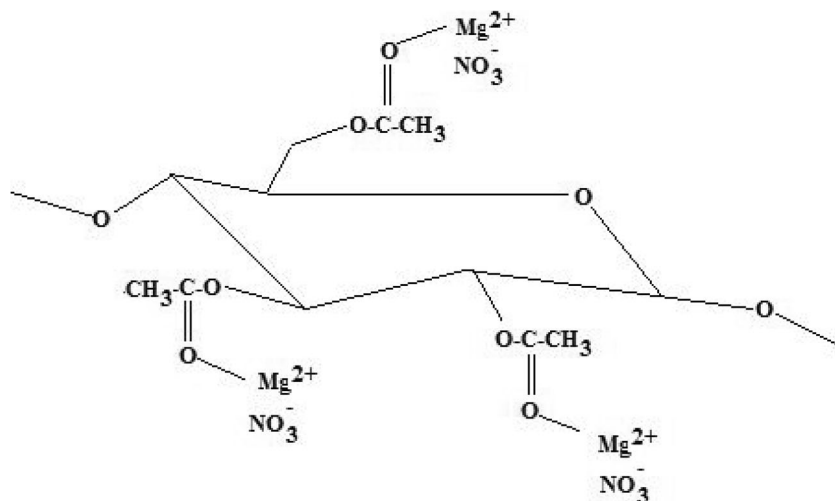


**Fig. 2** **a** FTIR spectrum for (a) pure CA, (b) 70 wt.%CA/30wt.%Mg(NO<sub>3</sub>)<sub>2</sub>·6H<sub>2</sub>O, (c) 60 wt.%CA/40 wt.%Mg(NO<sub>3</sub>)<sub>2</sub>·6H<sub>2</sub>O, and (d) 50 wt.%CA/50 wt.%Mg(NO<sub>3</sub>)<sub>2</sub>·6H<sub>2</sub>O in the range 1400–700 cm<sup>-1</sup>. **b** FTIR spectrum for (a) pure CA, (b) 70 wt.%CA/30 wt.%Mg(NO<sub>3</sub>)<sub>2</sub>·6H<sub>2</sub>O, (c) 60 wt.%CA/40 wt.%Mg(NO<sub>3</sub>)<sub>2</sub>·6H<sub>2</sub>O, and (d) 50 wt.%CA/50 wt.%Mg(NO<sub>3</sub>)<sub>2</sub>·6H<sub>2</sub>O in the range 1800–1500 cm<sup>-1</sup>

**Table 1** FTIR assignments of peaks observed for all prepared polymer electrolytes

Pure CA	70 wt.% CA/30 wt.% Mg(NO <sub>3</sub> ) <sub>2</sub> ·6H <sub>2</sub> O	60 wt.% CA/40 wt.% Mg(NO <sub>3</sub> ) <sub>2</sub> ·6H <sub>2</sub> O	50 wt.% CA/50 wt.% Mg(NO <sub>3</sub> ) <sub>2</sub> ·6H <sub>2</sub> O	Assignments
3387	3378	3358	3369	O–H stretching
1740	1737	1735	1732	C=O symmetric stretching
–	–	1646	1646	O–H bending
1368	1369	1371	1374	C–H bending and asymmetric stretching of NO <sub>3</sub> <sup>-</sup>
1221	1227	1228	1247	C–O stretching
1034	1035	1037	1024	C–O–C stretching
–	–	–	1076	Symmetric stretching of NO <sub>3</sub> <sup>-</sup>
906	902	900	895	O–H bending

**Fig. 3** Possible interaction between CA and  $\text{Mg}(\text{NO}_3)_2 \cdot 6\text{H}_2\text{O}$



compare with pure CA value. It reveals that the bond length has decreased, and hence, the frequency has increased.

Figure 3 shows the possible interaction between CA and  $\text{Mg}(\text{NO}_3)_2 \cdot 6\text{H}_2\text{O}$ . The interaction between the CA and  $\text{Mg}^{2+}$  ion of  $\text{Mg}(\text{NO}_3)_2 \cdot 6\text{H}_2\text{O}$  through the carbonyl group implies that the ions are mobile in the system. The high mobility of ions favors to the highest ionic conductivity. This confirms that  $\text{Mg}^{2+}$  of  $\text{Mg}(\text{NO}_3)_2 \cdot 6\text{H}_2\text{O}$  has the potential to function as the charge carrier in the system. The weakly bounded  $\text{Mg}^{2+}$  ion can hop through the coordinating site of the C=O of host polymer and the conduction takes place [24].

### Differential scanning calorimetry

Figure 4 shows the thermogram of pure CA and CA/ $\text{Mg}(\text{NO}_3)_2 \cdot 6\text{H}_2\text{O}$  complexes. The ( $T_g$ ) value for pure CA is 83.4 °C. A similar  $T_g$  value has been reported by Monisha et al. After the addition of salt  $\text{Mg}(\text{NO}_3)_2 \cdot 6\text{H}_2\text{O}$ , due to the plasticization effect of salt in the polymer structure, the  $T_g$  has shifted to lower values [8]. The  $T_g$  values obtained are 76.84 °C and 61.84 °C for the complexes of 70 wt.% CA/30 wt.%  $\text{Mg}(\text{NO}_3)_2 \cdot 6\text{H}_2\text{O}$  and 60 wt.% CA/40 wt.%  $\text{Mg}(\text{NO}_3)_2 \cdot 6\text{H}_2\text{O}$ , respectively. Similarly, Manjuladevi et al. have reported decreasing  $T_g$  values for increasing salt ratios for the samples of PVA/PAN/ $\text{Mg}(\text{NO}_3)_2$  and PVA/PAN/ $\text{Mg}(\text{ClO}_4)_2$ , Shanmugapriya et al. have reported  $T_g$  values

shifted to lower values with the addition of salt for the sample of I-Carrageenan/ $\text{Mg}(\text{ClO}_4)_2$ , and also, Mahalakshmi et al. have found the same result for CA/ $\text{Mg}(\text{ClO}_4)_2$  polymer membranes [18]. The decrease in  $T_g$  value with the addition of salt indicates disrupts of the crystallinity in the polymer CA. It creates maximum flexibility, and the ions are free to move into the polymer chain network [25]. It leads to higher segmental motion in the polymer electrolytes. Such segmental motion produces voids, which helps for a free flow of ions into the polymer matrix.

The further increase in the salt concentration for the 50 wt.% CA/50 wt.%  $\text{Mg}(\text{NO}_3)_2 \cdot 6\text{H}_2\text{O}$  electrolyte causes an increase in the value to 68.31 °C. The reason for increase of  $T_g$  value for 50 wt.% CA/50 wt.%  $\text{Mg}(\text{NO}_3)_2 \cdot 6\text{H}_2\text{O}$  electrolyte is due to decrease of amorphous nature. The decrease in the amorphous nature is evident from the XRD pattern of 50 wt.% CA/50 wt.%  $\text{Mg}(\text{NO}_3)_2 \cdot 6\text{H}_2\text{O}$ . The XRD pattern shows that the peaks appear due to CA again. So, it is natural to observe increase of  $T_g$  value for 50 wt.% CA/50 wt.%  $\text{Mg}(\text{NO}_3)_2 \cdot 6\text{H}_2\text{O}$ . The glass transition temperature for the various components of CA with  $\text{Mg}(\text{NO}_3)_2 \cdot 6\text{H}_2\text{O}$  has been listed in Table 3.

### Impedance analysis

Impedance spectroscopy is one of the powerful techniques to measure the ionic conductivity of the polymer material.

**Table 2** The force constant details for C–O stretching vibration for pure CA, 70 wt.% CA/30 wt.%  $\text{Mg}(\text{NO}_3)_2 \cdot 6\text{H}_2\text{O}$ , 60 wt.% CA/40 wt.%  $\text{Mg}(\text{NO}_3)_2 \cdot 6\text{H}_2\text{O}$ , and 50 wt.% CA/50 wt.%  $\text{Mg}(\text{NO}_3)_2 \cdot 6\text{H}_2\text{O}$  electrolytes

Polymer electrolytes	C–O stretching	
	Wavenumber ( $\text{cm}^{-1}$ )	Force constant (N/cm)
Pure CA	1221	6.00
70 wt.% CA/30 wt.% $\text{Mg}(\text{NO}_3)_2 \cdot 6\text{H}_2\text{O}$	1227	6.07
60 wt.% CA/40 wt.% $\text{Mg}(\text{NO}_3)_2 \cdot 6\text{H}_2\text{O}$	1228	6.08
50 wt.% CA/50 wt.% $\text{Mg}(\text{NO}_3)_2 \cdot 6\text{H}_2\text{O}$	1247	6.23

**Fig. 4** DSC thermogram glass transition temperature ( $T_g$ ) for **a** pure CA, **b** 70 wt.% CA/30 wt.%  $Mg(NO_3)_2 \cdot 6H_2O$ , **c** 60 wt.% CA/40 wt.%  $Mg(NO_3)_2 \cdot 6H_2O$ , and **d** 50 wt.% CA/50 wt.%  $Mg(NO_3)_2 \cdot 6H_2O$

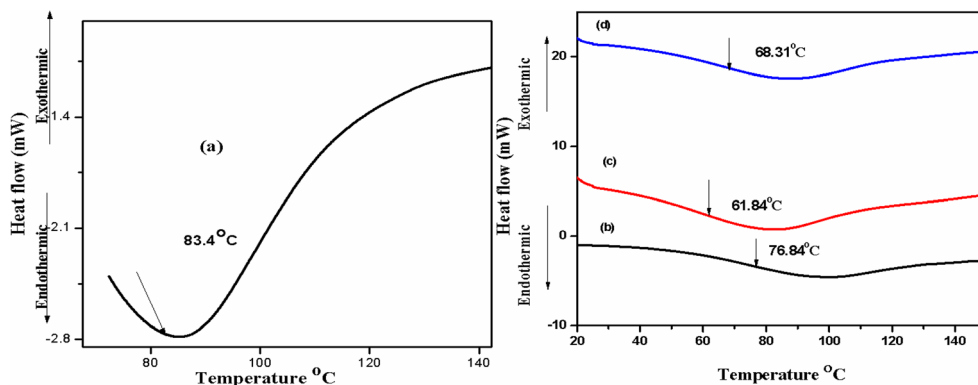


Figure 5 shows the cole-cole plot for the pure CA, 70 wt.% CA/30 wt.%  $Mg(NO_3)_2 \cdot 6H_2O$ , 60 wt.% CA/40 wt.%  $Mg(NO_3)_2 \cdot 6H_2O$ , and 50 wt.% CA/50 wt.%  $Mg(NO_3)_2 \cdot 6H_2O$  polymer electrolytes at room temperature (303 K) with a corresponding equivalent circuit. Generally, the cole-cole plot consists of a semicircle in the high-frequency region followed by an inclined spike in the low-frequency region. The high-frequency semicircle occurred due to the parallel combination of bulk resistance (due to migration of ions) and bulk capacitance (due to immobile polymer chain). The low-frequency spike is represented by a constant phase element. It is due to the formation of double-layer capacitance at the electrode-electrolyte interface [24]. In the present investigation, the semicircular portion is observed for pure CA. A total of 70 wt.% CA/30 wt.%  $Mg(NO_3)_2 \cdot 6H_2O$ , 60 wt.% CA/40 wt.%  $Mg(NO_3)_2 \cdot 6H_2O$ , and 50 wt.% CA/50 wt.%  $Mg(NO_3)_2 \cdot 6H_2O$  polymer electrolytes have only inclined spike and the semicircle was not observed, which indicates that the polymer electrolytes have resistive component only and the capacitive nature of electrolyte has vanished.

The bulk resistance ( $R_b$ ) of the polymer electrolytes has been calculated from the cole-cole plot using the Boukamp software [26]. The ionic conductivity ( $\sigma$ ) was calculated using the equation:

$$\sigma = t/R_b A \tag{3}$$

where  $t$  and  $A$  are the thickness and the area of the polymer electrolytes, respectively.

The Eq. (3) was used to measure the ionic conductivity for all samples at room temperature and listed in Table 4. The

highest ionic conductivity at room temperature determined as  $9.19 \times 10^{-4}$  S/cm for the 60 wt.% CA/40 wt.%  $Mg(NO_3)_2 \cdot 6H_2O$  ratio polymer electrolyte.

The ionic conductivity is related to the number of charge carrier ( $n$ ) and their mobility ( $\mu$ ) according to the following equation

$$\sigma = ne\mu \tag{4}$$

The ionic conductivity of the pure CA is  $3.1 \times 10^{-9}$  S/cm. The addition of  $Mg(NO_3)_2 \cdot 6H_2O$  with a polymer increases the number of charge carriers. It increases the ionic conductivity because the salt  $Mg(NO_3)_2 \cdot 6H_2O$  dissociates into  $Mg^{2+}$  and  $NO_3^-$  ions and producing more charge carriers. When 40 wt.% of  $Mg(NO_3)_2 \cdot 6H_2O$  added to the polymer, the maximum numbers of charge carriers produced. So, the conductivity reaches the highest value of  $9.19 \times 10^{-4}$  S/cm. It has a higher amorphous nature, it is confirmed by XRD. This membrane has got higher flexibility, it is confirmed by a low glass transition temperature.

The further addition of the  $Mg(NO_3)_2 \cdot 6H_2O$  salt over 50 wt.% CA/50 wt.%  $Mg(NO_3)_2 \cdot 6H_2O$  decreases the conductivity, due to the formation of more ion aggregates in the polymer [27].

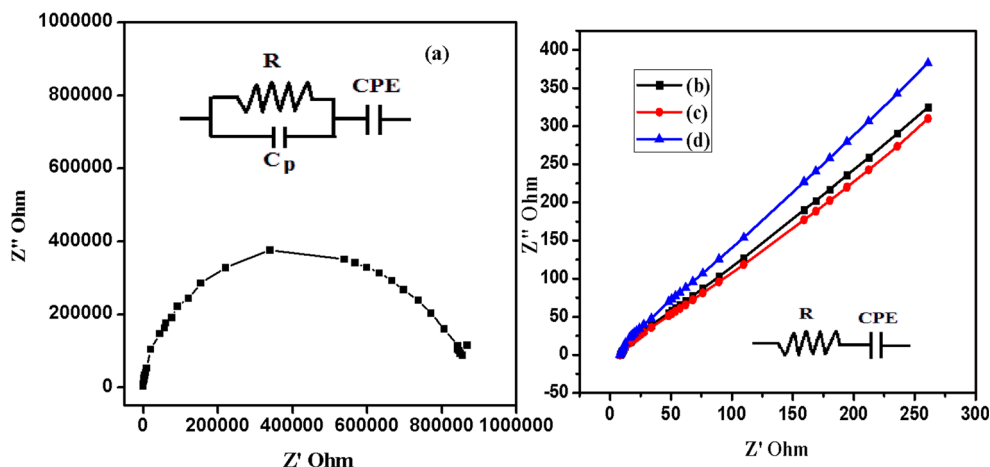
### Frequency-dependent conductivity

The frequency dependence of the conductivity measured for the pure CA and the CA with different composition of  $Mg(NO_3)_2 \cdot 6H_2O$  at room temperature is shown in Fig. 6. Due to electrode-electrolyte space charge polarization effects, the low-frequency dispersion region is produced [28]. The

**Table 3** Glass transition temperature for various composition of CA with  $Mg(NO_3)_2 \cdot 6H_2O$

Sl.no.	CA/ $Mg(NO_3)_2 \cdot 6H_2O$ composition (wt.%)	Glass transition temperature (°C)
1	Pure CA	83.4
2	70 wt.%CA/30 wt.% $Mg(NO_3)_2 \cdot 6H_2O$	76.84
3	60 wt.%CA/40 wt.% $Mg(NO_3)_2 \cdot 6H_2O$	61.84
4	50 wt.%CA/50 wt.% $Mg(NO_3)_2 \cdot 6H_2O$	68.31

**Fig. 5** **a** Cole-Cole plot for pure CA with a corresponding equivalent circuit. Cole-Cole plot for **b** 70 wt.% CA/30 wt.%  $\text{Mg}(\text{NO}_3)_2 \cdot 6\text{H}_2\text{O}$ , **c** 60 wt.% CA/40 wt.%  $\text{Mg}(\text{NO}_3)_2 \cdot 6\text{H}_2\text{O}$ , and **d** 50 wt.% CA/50 wt.%  $\text{Mg}(\text{NO}_3)_2 \cdot 6\text{H}_2\text{O}$  with corresponding equivalent circuit



plateau region corresponds to the dc conductivity ( $\sigma_{dc}$ ) of the PEs. The ( $\sigma_{dc}$ ) value calculated from extrapolating the plateau region to the log  $\sigma$  axis for all the samples. The 60 wt.% CA/40 wt.%  $\text{Mg}(\text{NO}_3)_2 \cdot 6\text{H}_2\text{O}$  sample has got the highest ionic conductivity. The ionic conductivity values obtained from the conduction spectra coincide with conductivity values derived from the cole-cole plot for all the samples.

## Transport number measurement

### Wagner's dc-polarization technique

Wagner (1957) proposed the dc polarization method to find out the ionic and electronic transference numbers [29]. In this method, the dc current monitored as a function of time on the application of a fixed dc voltage across the highest ionic conducting sample using stainless steel blocking electrodes. The electrolyte polarized by applying the dc potential of 1.5 V across the cell of SS/60 wt.% CA/40 wt.%  $\text{Mg}(\text{NO}_3)_2 \cdot 6\text{H}_2\text{O}$ /SS, which results in the movement of the mobile ions towards the blocking electrode. The transference number calculated by the formula

$$t_{\text{ion}} = (I_f - I_i) / I_i \quad (5)$$

where  $I_i$  is the initial and  $I_f$  the final current.

The polarization current monitored as a function of time. Figure 7 shows the initial current decreases with time. The total transference number ( $t_{\text{ion}}$ ) for the maximum conductivity

polymer 60 wt.% CA/40 wt.%  $\text{Mg}(\text{NO}_3)_2 \cdot 6\text{H}_2\text{O}$  is calculated as 0.98 using the Eq. (5), which is close to unity, so it means that only a negligible contribution comes from the electrons.

### Calculation of transport no. of $\text{Mg}^{2+}$ ion using Evan's method

The transport no. of  $\text{Mg}^{2+}$  ions in the PE system is obtained from a combination of AC and DC techniques, as proposed by Evans et al. [30]. In this method, the transport number  $t^+$  of  $\text{Mg}^{2+}$  ions for the highest conducting film was evaluated using the symmetrical cell  $\text{Mg}/60 \text{ wt.}\% \text{ CA}/40 \text{ wt.}\% \text{ Mg}(\text{NO}_3)_2 \cdot 6\text{H}_2\text{O}/\text{Mg}$ . The cell polarized by applying a DC voltage of 1.5 V.

Then, the initial ( $I_o$ ) and the final current ( $I_s$ ) values were derived from the current-time plot, as shown in Fig. 8. The cell resistance has recorded before and after the polarization by using the impedance measurement, and a graph plotted for corresponding values is shown in Fig. 8.

The transport number of  $\text{Mg}^{2+}$  is calculated using the formula

$$t^+ = I_s(\Delta V - R_o \times I_o) / I_o(\Delta V - R_s \times I_s) \quad (6)$$

where  $I_o$  and  $I_s$  are the initial and the final current,  $V$  is the applied dc voltage of 1.5 V, and  $R_o$  and  $R_s$  are the cell resistance before and after the polarization, respectively.

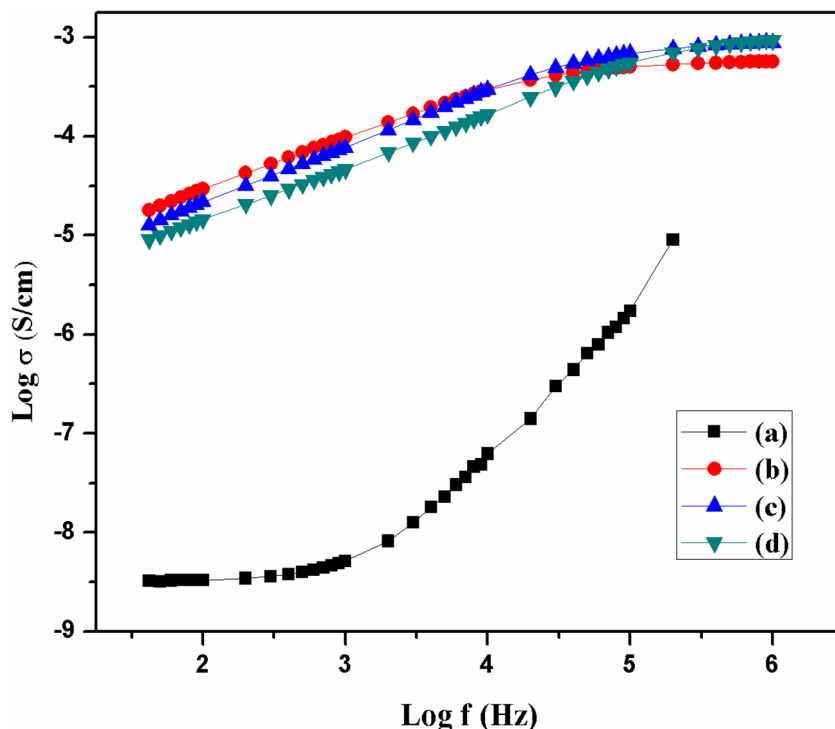
The value of the  $\text{Mg}^{2+}$  ion transport number was calculated to be 0.35 for the highest conducting film of the 60 wt.% CA/40 wt.%  $\text{Mg}(\text{NO}_3)_2 \cdot 6\text{H}_2\text{O}$  electrolyte. This value is a very

**Table 4** Ionic conductivity values of pure CA and CA doped with  $\text{Mg}(\text{NO}_3)_2 \cdot 6\text{H}_2\text{O}$

Sl.no.	CA/ $\text{Mg}(\text{NO}_3)_2 \cdot 6\text{H}_2\text{O}$ composition (wt.%)	Ionic conductivity S $\text{cm}^{-1}$
1	Pure CA	$3.1 \times 10^{-9}$
2	70 wt.% CA/30 wt.% $\text{Mg}(\text{NO}_3)_2 \cdot 6\text{H}_2\text{O}$	$1.89 \times 10^{-5}$
3	60 wt.% CA/40 wt.% $\text{Mg}(\text{NO}_3)_2 \cdot 6\text{H}_2\text{O}$	$9.19 \times 10^{-4}$
4	50 wt.% CA/50 wt.% $\text{Mg}(\text{NO}_3)_2 \cdot 6\text{H}_2\text{O}$	$1.33 \times 10^{-4}$



**Fig. 6** Frequency dependence conduction spectra for **a** pure CA, **b** 70 wt.% CA/30 wt.% Mg(NO<sub>3</sub>)<sub>2</sub>·6H<sub>2</sub>O, **c** 60 wt.% CA/40 wt.% Mg(NO<sub>3</sub>)<sub>2</sub>·6H<sub>2</sub>O, and **d** 50 wt.% CA/50 wt.% Mg(NO<sub>3</sub>)<sub>2</sub>·6H<sub>2</sub>O



close agreement with the value of 0.31. It was measured for the highest ionic conducting polymer electrolyte of 40 wt.% CA/60 wt.% Mg(ClO<sub>4</sub>)<sub>2</sub> by Mahalakshmi et al. [18]. Mangalam et al. have reported a value of 0.31 for the composition of 50 wt.% PVA/50 wt.% PVP with 25 wt.% Mg(ClO<sub>4</sub>)<sub>2</sub>. Kumar et al. have studied the PMMA-based GPE system with the Mg(CF<sub>3</sub>SO<sub>3</sub>)<sub>2</sub> salt and reported a value of 0.33. Manjuladevi et al. have reported the value as 0.30 for the transport number of the Mg<sup>2+</sup> ions in their work for the 92.5 wt.% PVA/7.5 wt.% PAN with the 0.3 wt.% Mg(NO<sub>3</sub>)<sub>2</sub>

electrolyte. A total of 0.26 has been reported as transport number of the Mg<sup>2+</sup> by Sangeetha et al. for the K-Carrageenan 1 g/0.6 wt.% MgCl<sub>2</sub>. Kiruthika et al. developed the polymer electrolyte film based on pectin with magnesium nitrate and calculated the transport number of Mg<sup>2+</sup> ions as 0.29.

**Linear sweep voltammetry**

Electrochemical stability is an essential one to determine the long-term performance of electrochemical devices. The

**Fig. 7** D.C. polarization curve of **a** SS/60 wt.% CA/40 wt.% Mg(NO<sub>3</sub>)<sub>2</sub>·6H<sub>2</sub>O/SS cell and **b** Mg/60 wt.% CA/40 wt.% Mg(NO<sub>3</sub>)<sub>2</sub>·6H<sub>2</sub>O/Mg cell at room temperature

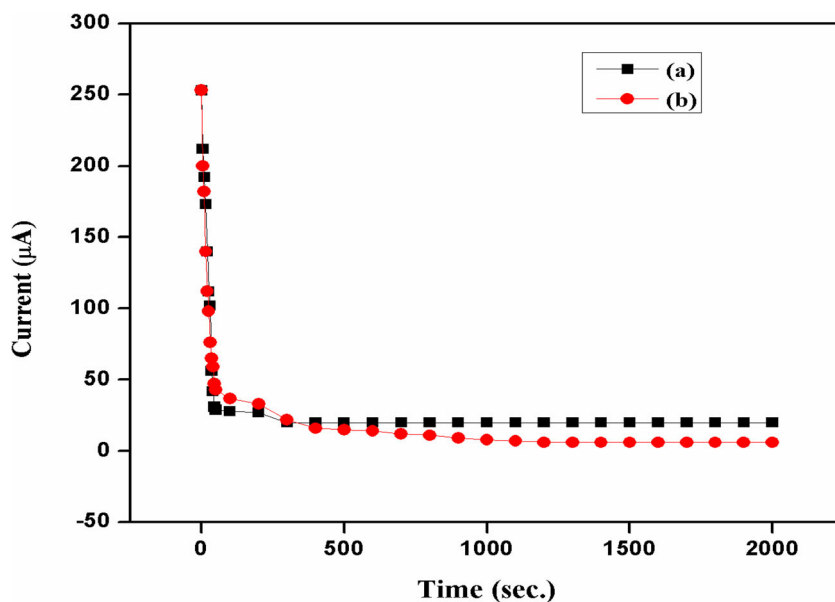
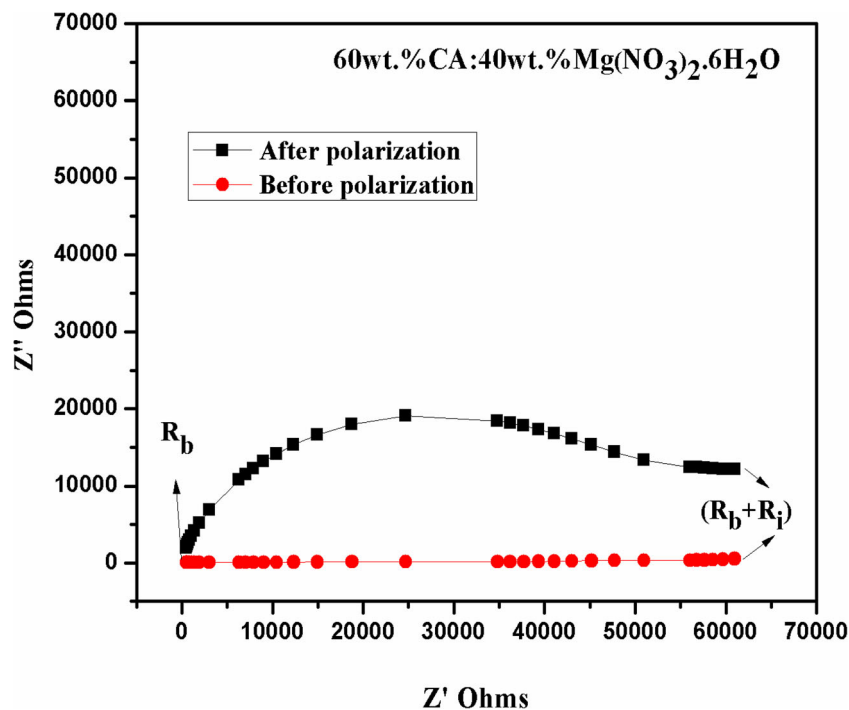


**Fig. 8** Cole-Cole plot before and after polarization of a typical symmetric Mg/60 wt.% CA/40 wt.% Mg(NO<sub>3</sub>)<sub>2</sub>·6H<sub>2</sub>O/Mg cell at room temperature



highest conducting polymer electrolyte 60 wt.% CA/40 wt.% Mg(NO<sub>3</sub>)<sub>2</sub>·6H<sub>2</sub>O has been used to study electrochemical stability at room temperature by linear sweep voltammetry (LSV). LSV was recorded for SS/60 wt.% CA/40 wt.% Mg(NO<sub>3</sub>)<sub>2</sub>·6H<sub>2</sub>O/SS at a scan rate of 5 mV s<sup>-1</sup>. Figure 9 shows the current-voltage response curve. The anodic decomposition limit of the polymer electrolyte was considered as the voltage at which the current flows through the system [31]. A sudden rise in the current was observed from the graph at 3.65 V. This value is called an electrochemical stability value, which is assumed to be

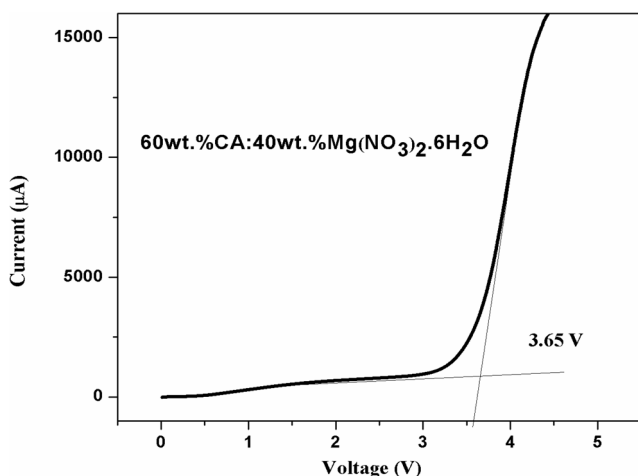


**Fig. 9** Linear sweep voltammetry of SS/60 wt.% CA/40 wt.% Mg(NO<sub>3</sub>)<sub>2</sub>·6H<sub>2</sub>O/SS cell recorded at a scan rate of 5 mV s<sup>-1</sup> at room temperature

the breakdown voltage of the polymer electrolyte. This result suggests that the prepared electrolyte is suitable for its application in Mg ion batteries. Osman et al. have reported the stability value of 3.5 V for the SS/PVDF-HFP/20 wt.% Mg(CF<sub>3</sub>SO<sub>3</sub>)<sub>2</sub>/Mg. Manjuladevi et al. reported electrochemical stability value of 3.4 V for the 92.5 wt.% PVA/7.5 wt.% PAN/0.3 wt.% Mg(NO<sub>3</sub>)<sub>2</sub> polymer electrolyte. The electrochemical stability value of 3.8 V has been obtained by Kiruthika et al. for 50 wt% pectin/50 wt% Mg(NO<sub>3</sub>)<sub>2</sub> electrolyte membrane. Sangeetha et al. have measured electrochemical stability value to be 1.94 V for the highest ionic conducting electrolyte of K-Carrageenan 1 g/0.6 wt% MgCl<sub>2</sub>. Mahalakshmi et al. have reported electrochemical stability value as 3.58 V for the highest ionic conducting polymer membrane 40 wt.% CA/60 wt.% Mg(ClO<sub>4</sub>)<sub>2</sub> [17].

### Cyclic voltammetry studies

Mg/SPE/Mg symmetric cell is constructed using highest conducting polymer electrolyte 60 wt.% CA/40 wt.% Mg(NO<sub>3</sub>)<sub>2</sub>·6H<sub>2</sub>O. It was subjected to cyclic voltammetry between -5 and +5 V at a scan rate of 1 mV s<sup>-1</sup>, and it is shown in Fig. 10. The cathodic and anodic peaks are distinctly observed [32].

### Construction and performance of the Mg battery cell

A primary magnesium battery was constructed using the highest ionic conductivity polymer electrolyte (60 wt.%

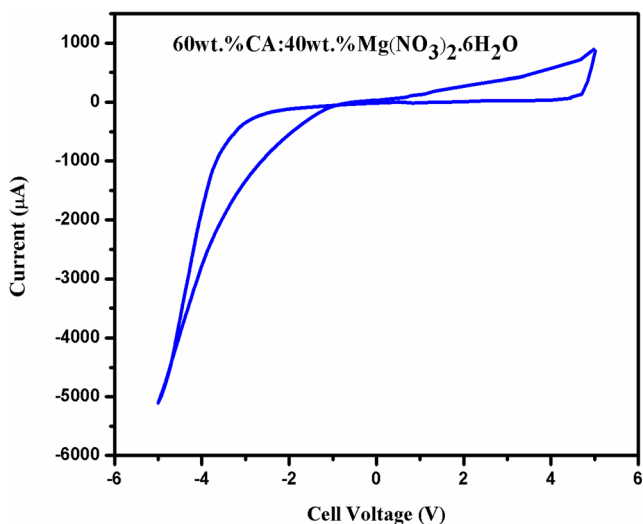


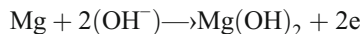
**Fig. 10** Cyclic voltammetry for 60 wt.% CA/40 wt.% Mg(NO<sub>3</sub>)<sub>2</sub>·6H<sub>2</sub>O polymer electrolyte

CA/40 wt.% Mg(NO<sub>3</sub>)<sub>2</sub>·6H<sub>2</sub>O). The electrolyte is sandwiched between the anode and the cathode in the battery holder. Figure 10a shows the schematic diagram of the fabricated battery. The initial open-circuit voltage (OCV) recorded as 2.23 V, and the OCV has monitored with time. After 1 day, the OCV was reduced slightly to 2.1 V, which remains at the same value for 7 subsequent days, as shown in Fig. 10b.

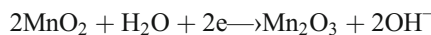
This small intermediate drop occurred in battery voltage due to the cell formation reactions at the electrodes

[24]. The chemical reactions taking place in the battery cell are the following:

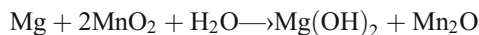
At the anode



At the cathode



Overall reaction



The presence of OH ion in the membrane is known as occluded moisture/water. The occluded water is a type of non-essential water that retained due to the physical force in microscopic pores, spaced irregularly throughout the solid polymer CA [33].

The external load 100 kΩ has connected to the circuit for the measurement of the battery discharge characteristic at room temperature. Figure 11c shows the discharge behavior of the battery. Due to the polarization effect at the electrolyte-electrode interface, the potential of the battery decreases initially, and it remains constant at 1.86 V, which observed for 1 week.

**Fig. 11** a Schematic diagram of battery configuration. b Open circuit potential as a function of time for 60 wt.% CA/40 wt.% Mg(NO<sub>3</sub>)<sub>2</sub>·6H<sub>2</sub>O polymer electrolyte. c Discharge curves of cell using 100 KΩ for 60 wt.% CA/40 wt.% Mg(NO<sub>3</sub>)<sub>2</sub>·6H<sub>2</sub>O polymer electrolyte

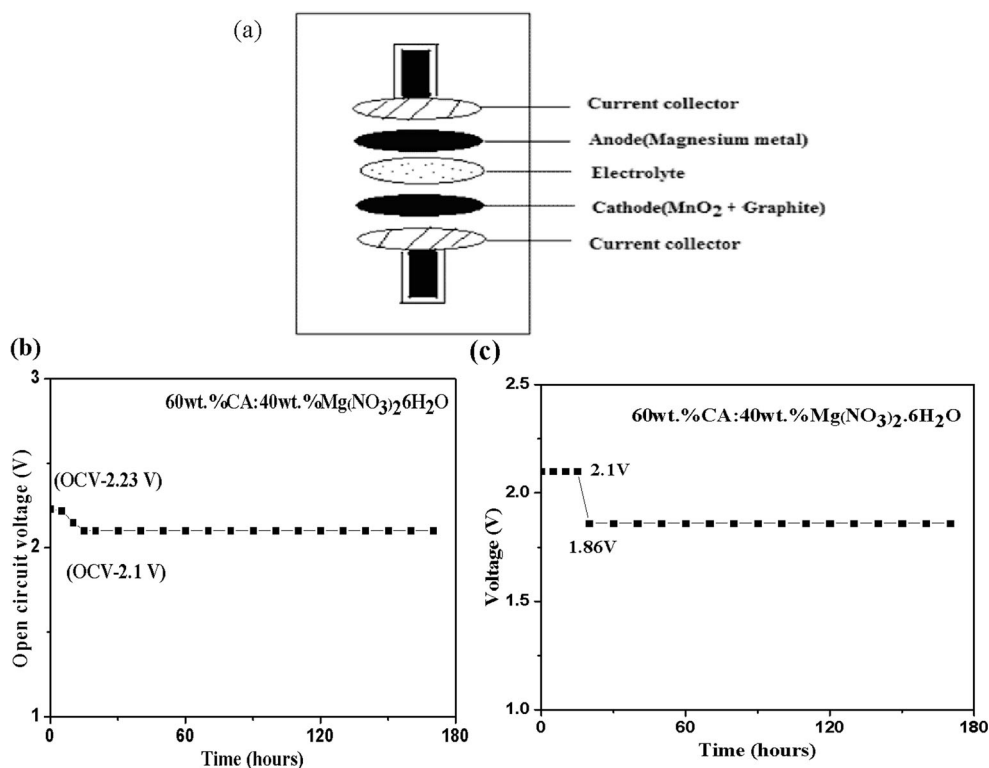


**Table 5** Battery parameters

Specification of cell parameters	Values of battery parameters
Electrolyte area (cm <sup>2</sup> )	1.15
Battery weight (g)	1.18
Effective electrolyte diameter (cm)	1.2
Battery thickness (cm)	0.25
Open circuit voltage (V)	2.1
Cut off potential (h)	170
Current drawn (μA)	53

The battery cell parameters have been listed in Table 5.

## Conclusion

A new solid polymer electrolyte CA with various concentrations of Mg(NO<sub>3</sub>)<sub>2</sub>·6H<sub>2</sub>O has been prepared and characterized. The XRD patterns reveal that the inclusion of Mg(NO<sub>3</sub>)<sub>2</sub>·6H<sub>2</sub>O change the semi-crystalline nature of the polymer to more amorphous. The prepared membranes are subjected to the FTIR analysis. The DSC studies indicate that the glass transition temperature decreases with the increase of Mg(NO<sub>3</sub>)<sub>2</sub>·6H<sub>2</sub>O salt concentration. The highest ionic conductivity has been achieved for the 60 wt.% CA/40 wt.% Mg(NO<sub>3</sub>)<sub>2</sub>·6H<sub>2</sub>O membrane as  $9.19 \times 10^{-4}$  S/cm using Ac-impedance analysis at room temperature. Using Evan's method, the ionic transference number for Mg<sup>+</sup> has been estimated as 0.35 for the 60 wt.% CA/40 wt.% Mg(NO<sub>3</sub>)<sub>2</sub>·6H<sub>2</sub>O electrolyte film. The electrochemical stability is estimated using LSV as 3.65 V, which is sufficient for electrochemical applications. A primary magnesium battery has been constructed using the highest ionic conducting membrane 60 wt.% CA/40 wt.% Mg(NO<sub>3</sub>)<sub>2</sub>·6H<sub>2</sub>O, and its performance was studied. The open circuit voltage (OCV) of the battery is found as 2.23 V.

**Acknowledgments** Authors are thankful to Dr. RAJKUMR, Department of Chemistry, Vivekananda College, Thiruvudagam, Madurai and to Dr. K. VIGNESHWARI, Department of Chemistry, Sri Meenakshi Govt. Arts College for women, Madurai for their useful discussion with regard to FTIR spectral analysis.

## References

- Ye L, Feng Z (2010) Polymer electrolytes fundamentals and applications 551 © Wood head publishing Limited
- Mohiuddin M, Kumar B, Haque S (2017) Biopolymer composites in photovoltaics and photodetectors. *Biopolymer Composites in Electronics*:459–486. <https://doi.org/10.1016/b978-0-12-809261-3.00017-6>
- Mohanty AK et al. (2005) Natural fibers. *Biopolymers and Biocomposites* © CRC press
- McCray B, Vilker VL, Nobe K (1991) Reverse osmosis cellulose acetate membranes II dependence of transport properties on acetyl content. *J Membr Sci* 59(3):317–330. [https://doi.org/10.1016/s0376-7388\(00\)80820-0](https://doi.org/10.1016/s0376-7388(00)80820-0)
- Abidin SZZ, Ali AMM, Hassan OH, Yahya MZA (2013) Electrochemical studies on cellulose acetate-LiBOB polymer gel electrolytes. *Int J Electrochem Sci* 8:7320–7326
- Monisha S, Selvasekarapandian S, Mathavan T, Milton Franklin Benial A, Manoharan S, Karthikeyan S (2016) Preparation and characterization of biopolymer electrolyte based on cellulose acetate for potential applications in energy storage devices. *J Mater Sci Mater Electron* 27(9):9314–9324
- Monisha S, Mathavan T, Selvasekarapandian S, Milton Franklin Benial A, Aristatil G, Premalatha M, Vinoth Pandi D (2017) Investigation of biopolymer electrolyte based on cellulose acetate-ammonium nitrate for potential use in electrochemical devices. *Carbohydr Polym* 157:38–47
- Monisha S, Mathavan T, Selvasekarapandian S, Benial AMF, Latha MP (2016) Preparation and characterization of cellulose acetate and lithium nitrate for advanced electrochemical devices. *Ionics* 23(10):2697–2706
- Ramesh S, Shanti R, Morris E (2012) Plasticizing effect of 1-allyl-3-methylimidazolium chloride in cellulose acetate based polymer electrolytes. *Carbohydr Polym* 87(4):2624–2629. <https://doi.org/10.1016/j.carbpol.2011.11.037>
- Selvakumar M, Bhat DK (2008) LiClO<sub>4</sub> doped cellulose acetate as a biodegradable polymer electrolyte for supercapacitors. *J Appl Polym Sci* 110(1):594–602
- Sarangika HNM, Dissanayake MAKL, Senadeera GKR, Rathnayake RRDV, Pitawala HMJC (2017) Polyethylene oxide and ionic liquid-based solid polymer electrolyte for rechargeable magnesium batteries doi: <https://doi.org/10.1007/s11581-016-1870-3>
- Kim HS, Arthur TS, Allred GD, Zajicek J, Newman JG, Rodnyansky AE, Oliver AG, Boggess WC, Muldoon J (2011) Structure and compatibility of a magnesium electrolyte with a sulphur cathode. *Nat Commun* 2:427
- Pandey GP, Agrawal RC, Hashmi SA (2009) Magnesium ion-conducting gel polymer electrolytes dispersed with nanosized magnesium oxide. *J Power Sources* 190(2):563–572. <https://doi.org/10.1016/j.jpowsour.2009.01.057>
- Manjuladevi R, Selvasekarapandian S, Thamilselvan M, Mangalam R, Monisha S, Selvin PC (2018) A study on blend polymer electrolyte based on poly(vinyl alcohol)-poly (acrylonitrile) with magnesium nitrate for magnesium battery. *Ionics*. 24:3493–3506. <https://doi.org/10.1007/s11581-018-2500-z>
- Shanmuga Priya S, Karthika M, Selvasekarapandian S, Manjuladevi R, Monisha S (2018) Study of biopolymer I-carrageenan with magnesium perchlorate. *Ionics* 24:3861–3875. <https://doi.org/10.1007/s11581-018-2535-1>
- Kiruthika S, Malathi M, Selvasekarapandian S, Tamilarasan K, Moniha V, Manjuladevi R (2019) Eco-friendly biopolymer electrolyte, pectin with magnesium nitrate salt, for application in electrochemical devices. *J Solid State Electrochem* 23:2181–2193. <https://doi.org/10.1007/s10008-019-04313-6>
- Sangeetha P, Selvakumari TM, Selvasekarapandian S, Srikumar SR, Manjuladevi R, Mahalakshmi M (2019) Preparation and characterization of biopolymer K-carrageenan with MgCl<sub>2</sub> and its application to electrochemical devices. *Ionics*. 26:233–244. <https://doi.org/10.1007/s11581-019-03193-0>
- Mahalakshmi M, Selvanayagam S, Selvasekarapandian S, Moniha V, Manjuladevi R, Sangeetha P (2019) Characterization of biopolymer electrolytes based on cellulose acetates with magnesium

- perchlorate ( $\text{Mg}(\text{ClO}_4)_2$ ) for energy storage devices. *J Sci Adv Mater Devices* 4:276–284. <https://doi.org/10.1016/j.jsamd.2019.04.006>
19. Shuhaimi NEA, Alias NA, Kufian MZ, Majid SR, Arof AK (2010) Characteristics of methyl cellulose- $\text{NH}_4\text{NO}_3$ -PEG electrolyte and application in fuel cells. *J Solid State Electrochem* 14(12):2153–2159. <https://doi.org/10.1007/s10008-010-1099-4>
  20. Hodge RM, Edward GH, Simon GP (1996) Water absorption and states of water in semi crystalline poly (vinyl alcohol) films. *Polymer* 37(8):1371–1376
  21. Samsudin AS, Khairul WM, Isa MIN (2012) Characterization on the potential of carboxy methylcellulose for application as proton conducting biopolymer electrolytes. *J Non-Cryst Solids* 358(8): 1104–1112. <https://doi.org/10.1016/j.jnoncrsol.2012.02.004>
  22. Koenig JL (1999) *Spectroscopy of polymers* © Amsterdam: Elsevier 2nd ed
  23. Sulaiman M, Rahman AA, Mohamed NS (2013) Structural, thermal and conductivity studies of magnesium nitrate – alumina composite solid electrolytes prepared via sol-gel method. *Int J Electrochem Sci*, 6647–6655
  24. Prajapati GK, Gupta PN (2011) Comparative study of the electrical and dielectric properties of PVA–PEG– $\text{Al}_2\text{O}_3$ –MI (M=Na, K, Ag) complex polymer electrolytes. *Phys B Condens Matter* 406(15–16): 3108–3113. <https://doi.org/10.1016/j.physb.2011.05.019>
  25. Vargas MA, Vargas RA, Mellander BE (2000) More studies on the PVAI+ $\text{H}_3\text{PO}_2$ + $\text{H}_2\text{O}$  proton conductor gels. *Electrochim Acta* 45(8–9):1399–1403. [https://doi.org/10.1016/s0013-4686\(99\)00350-3](https://doi.org/10.1016/s0013-4686(99)00350-3)
  26. Boukamp BA (1986a) A nonlinear least squares fit procedure for analysis of immittance data of electrochemical systems. *Solid State Ionics* 20:31–44
  27. Ramya CS, Selvasekarapandian S, Savitha T, Hirankumar G, Baskaran R, Bhuvaneswari MS, Angelo PS (2006) Conductivity and thermal behavior of proton conducting polymer electrolyte based on poly (N-vinyl pyrrolidone). *Eur Polym J* 42(10):2672–2677
  28. Ramesh S, Shanti R, Morris E (2011) Discussion on the influence of DES content in CA-based polymer electrolytes. *J Mater Sci* 47(4):1787–1793. <https://doi.org/10.1007/s10853-011-5964-z>
  29. Wagner JB, Wagner CJ (1957) *Chem Rev* 26-597
  30. Evans J, Vincent CA, Bruce PG (1987) Electrochemical measurement of transference numbers in polymer electrolytes. *Polymer* 28(13):2324–2328
  31. Tiankhoon L, Ataollahi N, Hassan N H, Ahamad A (2015) *J Solid State Electrochem* 015–3017-2
  32. Kumar Y, Hashmi SA, Pandey GP (2011) Ionic liquid mediated magnesium ion conduction in poly(ethylene oxide) based polymer electrolyte. *Electrochim Acta* 56:3864–3873. <https://doi.org/10.1016/j.electacta.2011.02.035>
  33. Hambali D, Zainol NH, Othman L, Md Isa KB, Osman Z (2018) Magnesium ion conducting gel polymer electrolytes based on poly(vinylidene chloride-co-acrylonitrile) (PVdC-co-AN): a comparative study between magnesium trifluoromethane sulfonate ( $\text{MgTf}_2$ ) and magnesium bis(trifluoromethanesulfonimide) ( $\text{Mg}(\text{TFSI})_2$ ). *Ionics* 15–18

**Publisher's note** Springer Nature remains neutral with regard to jurisdictional claims in published maps and institutional affiliations.